

(t, p) reaction.

In summary, I find that a general treatment of the octupole-octupole particle-hole residual interaction provides a natural, unforced explanation for the low-lying 0^+ excited states in the light U isotopes (and Th isotones).

I thank Professors I. Hamamoto and A. Bohr for stimulating conversations on this problem. This work was performed under the auspices of the Division of Nuclear Physics of the U. S. Department of Energy.

¹K. Neergård and P. Vogel, Nucl. Phys. **A149**, 217 (1970).

²P. Vogel, Nucl. Phys. **A112**, 583 (1968).

³P. Möller, S. G. Nilsson, and R. K. Sheline, Phys.

Lett. **40B**, 329 (1972).

⁴R. R. Chasman, I. Ahmad, A. M. Friedman, and J. R. Erskine, Rev. Mod. Phys. **49**, 833 (1977).

⁵R. E. Griffin, A. D. Jackson, and A. B. Volkov, Phys. Lett. **36B**, 281 (1971); W. I. Van Rij and S. H. Kahana, Phys. Rev. Lett. **28**, 50 (1972).

⁶I. Ragnarsson and R. A. Broglia, Nucl. Phys. **A263**, 315 (1976).

⁷R. R. Chasman, Phys. Rev. C **15**, 1935 (1976).

⁸R. R. Chasman and W. Ogle, Nucl. Phys. **A303**, 67 (1978).

⁹R. R. Chasman, Phys. Rev. Lett. **28**, 1275 (1972).

¹⁰D. L. Hill and J. A. Wheeler, Phys. Rev. **89**, 1102 (1953).

¹¹D. M. Brink and A. Weiguny, Phys. Lett. **26B**, 497 (1968).

¹²F. K. McGowan *et al.*, Phys. Rev. C **10**, 1146 (1974).

¹³J. V. Maher *et al.*, Phys. Rev. Lett. **25**, 302 (1970);

J. V. Maher *et al.*, Phys. Rev. C **5**, 1380 (1972).

¹⁴R. F. Casten *et al.*, Phys. Lett. **40B**, 333 (1972).

Structure in Backward-Angle Excitation Functions for Strongly Absorbed Particles

S. Landowne

Sektion Physik, Universität München, D-8046 Garching, Germany

(Received 29 December 1978)

A strong, isolated pole gives rise to periodic structure in backward-angle excitation functions. A moderate pole interfering with a nonresonant diffraction amplitude produces similar structure. The $^{16}\text{O} + ^{28}\text{Si}$ backward-angle elastic excitation function is analyzed from these points of view.

Recent measurements by Braun-Munzinger *et al.*¹ revealed a large, oscillatory angular distribution in the backward direction for $^{16}\text{O} + ^{28}\text{Si}$ elastic scattering. This discovery generated considerable interest.² A number of papers investigating the experimental and theoretical ramifications of this phenomenon have subsequently appeared.²⁻¹¹

Barrette *et al.*⁴ measured excitation functions for $^{16}\text{O} + ^{28}\text{Si}$ and $^{12}\text{C} + ^{28}\text{Si}$ at extreme backward angles and observed some gross structure. Additional backward-angle excitation measurements are reported by Clover *et al.*⁵ and Renner *et al.*⁹ Dehnhard *et al.*⁶ fitted the elastic $^{16}\text{O} + ^{28}\text{Si}$ excita-

tion function by introducing a parity dependence into the optical potential. On the other hand Lee,⁸ based on a more conventional optical-model calculation, has interpreted the structure of the excitation function in terms of interference between internal and surface-barrier waves—as it was done for the case of α scattering.¹² Here I discuss a simple, rather general interpretation of structures in backward-angle excitation functions for strongly absorbed particles. At present, I consider only elastic scattering and focus on the $^{16}\text{O} + ^{28}\text{Si}$ data.

The amplitude for the elastic scattering of spinless, nonidentical nuclei is given by

$$f(\theta) = \frac{1}{2ik} \sum_{l=0}^{\infty} (2l+1) [\exp(i2\sigma_l) S_l - 1] P_l(\cos\theta), \quad (1)$$

where S_l is the nuclear partial-wave S matrix and

$$\exp(i2\sigma_l) = \Gamma(l+1+i\eta) / \Gamma(l+1-i\eta) \quad (2)$$

is the Coulomb partial S matrix, η being the Coulomb strength parameter. Now at $\theta = \pi$, $P_l(\cos\pi) = (-1)^l$ so that Eq. (1) becomes a sum of alternating terms. It can then be expressed in terms of a contour in-

tegral in the complex l plane which encloses the origin and the positive real axis as follows:

$$f(\pi) = \frac{1}{2\pi i} \oint_c dl \frac{\pi}{\sin \pi l} \frac{(2l+1)}{2ik} \{ \exp[i2\sigma(l)] S(l) - 1 \} - \sum_n \frac{\pi}{\sin \pi l_n} \frac{(2l_n+1)}{2ik} \exp[i2\sigma(l_n)] \beta_n, \quad (3)$$

where we also enclose some of the poles l_n of $S(l)$ lying in the first quadrant of the l plane. Thus β_n is the residue of $S(l)$ taken at the pole l_n . Equation (3) is a special case of the Watson-Sommerfeld technique of replacing partial-wave sums by integrals.^{7, 13-17}

I assume that the poles appearing in Eq. (3) govern the variation of $S(l)$ along the real axis in the general vicinity of the grazing partial wave L . The main part of the "background" integral contribution should then describe the classical scattering of low partial waves to the backward direction. This, in turn, is inhibited under the condition of strong absorption. To be more precise, assuming that S_l varies slowly for the low partial waves, the stationary phase contribution to Eq. (1) for the backward angles is

$$f^{\text{SP}}(\theta) = f_C(\theta) S_{l(\theta)} \approx -(\eta/2k) \exp(i2\sigma_0) S_0, \quad (4)$$

where f_C is the Coulomb amplitude and $l(\theta) \approx \eta(\pi - \theta)/2$. Assuming an exponential decay from the grazing L , one obtains

$$S_{l(\theta)} \sim \exp\{-[L - l(\theta)]/\Delta\} \sim \exp(-L/\Delta). \quad (5)$$

Typically such amplitudes are negligible.¹⁴

On the other hand, the pole terms describe diffraction scattering which, for backward angles, corresponds to surface partial waves which creep around the strong-absorption region.¹⁷ These waves are always relatively important for the cross section at $\theta = \pi$ since one sees the coherent (glory) scattering from the entire solid angle subtended by the edge of the strong-absorption region. Their contribution can be enhanced if there is a weak surface absorption or if a quasibound structure is formed during the collision. Thus large surface diffraction scattering in the backward direction suggests that particular poles are playing an important role.^{1, 15-17}

Consider then the contribution from a single pole located at $L + i\lambda$ where L is close to the grazing-partial-wave number while $\lambda > 0$ is small. We obtain

$$f^{\text{P}}(\pi) = \frac{-\pi\beta}{\sin[\pi(L+i\lambda)]} \frac{2L+1}{2ik} \exp(i2\sigma_L) \exp(-\lambda\theta_L^{\text{C}}), \quad (6)$$

where θ_L^{C} is the Coulomb deflection angle,

$$\theta_L^{\text{C}} = 2(d\sigma/dl)|_L = 2 \tan^{-1}[\eta/(L + \frac{1}{2})], \quad (7)$$

Thus for the backward-angle cross section, taken with respect to the Rutherford value, we have the one-pole result,

$$\frac{\sigma_{\text{P}}(\pi)}{\sigma_{\text{R}}(\pi)} = \left[\frac{|\beta| \pi(2L+1)}{\eta} \right]^2 \frac{\exp(-2\lambda\theta_L^{\text{C}})}{\sin^2(\pi L) + \sinh^2(\pi\lambda)}. \quad (8)$$

Accordingly, periodic structure will be observed in the excitation function as L changes by integer values, provided λ remains small ($\lambda \lesssim 0.5$). The peaks correspond to integer L values. Note that for such small λ values, the scale of the average cross section is fixed by $|\beta|^2$. The characteristic pole dependence shown by Eq. (8) has been recently noted by Fuller¹⁸ in a different context. Fuller¹⁸ has pointed out that such small λ values correspond to surface waves with life angles of $\sim 180^\circ$ —a fact which is sympathetic to the backward-angle amplitude.

A fit to the measured $^{16}\text{O} + ^{28}\text{Si}$ excitation function⁴ using Eq. (8) is shown by the solid line in

Fig. 1. I let L be proportional to the square root of the energy.^{15, 16} This fixes the structure frequency at $\Delta E \approx 2E/L$. I took $L = 22$ at 32 MeV as suggested by fits to the corresponding backward angular distribution.^{2, 4} To fix the scale, β must be small. I arbitrarily let $|\beta| = 1/(2L+1)$. A linear dependence was assumed for λ (Ref. 16) which was determined by adjusting the magnitudes of the peaks at 26.5 and 29.3 MeV. The result was $\lambda = 0.30, 0.34$, respectively.

It is striking that the positions of the maxima and minima are well reproduced by fixing one parameter. Note that the absolute L value is not so

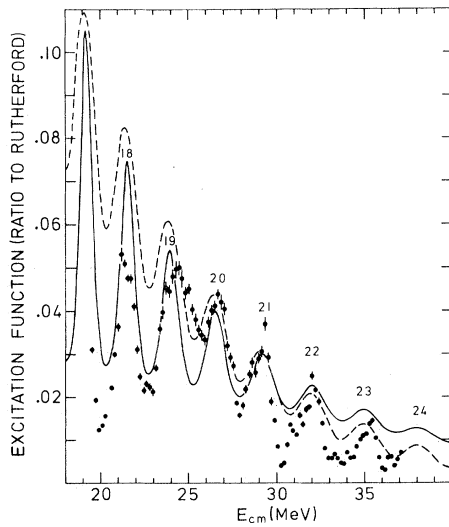


FIG. 1. Backward-angle excitation function for $^{16}\text{O} + ^{28}\text{Si}$ elastic scattering. The data are from Ref. 4 and include an angular range of $\theta_{\text{c.m.}} = 180 \pm 5^\circ$. The calculations show two types of pole dominance. The solid line results from a single, quasimolecular-type trajectory which is quite close to the real axis. The dashed curve results from a potential-barrier-type trajectory interfering with a nonresonant diffraction to amplitude.

well determined since Eq. (8) is rather stable with respect to small integer changes in L . Thus there is fair agreement with the L values of 17 ± 1 and 24 ± 1 determined for the 26 and 35 MeV peaks but an unacceptable comparison with the value $L = 9 \pm 1$ for the 21-MeV peak.⁴ This result seems to rule out a single-pole-trajectory interpretation of the excitation function at the lower energies.¹⁹

$$f^{\text{NR}}(\pi) = [\pi\Delta(2L+1)/k] \exp[i2(\sigma_L + \delta_L)] \exp(-\pi^2\Delta) [\exp(i\pi L) \exp(-\pi\Delta\theta_L) - \exp(-i\pi L) \exp(\pi\Delta\theta_L)]. \quad (11)$$

Here I used the two closest poles and have included the nuclear deflection in $\theta_L = \theta_L^{\text{C}} + 2d\delta_L/dL$.

Some time ago Frahn and Venter²³ (p. 274) obtained a similar expression using the Poisson summation technique. They noted that in the high-energy limit, $\theta_L \rightarrow 0$, one obtains periodic structure proportional to $\sin^2\pi l$. This result has also been recently discussed on a more general basis by Strutinsky.¹¹ However, because of the strong Coulomb deflection, this limit is not appropriate for typical heavy-ion scattering. (Takigawa and Lee¹² use a similar equation to discuss "barrier-wave" backward-angle α scattering.) Note that the nuclear deflection for the grazing L is usually small. This is evidenced by the validity of the Blair quarter-point recipe ($\theta_L = \theta_{L4}$) which ignores nuclear scattering.

For $\theta_L > 0$ only the second term of Eq. (11), corresponding to a parametrized pole below the real axis, is relevant. Interference of this term with a physical pole having $\lambda > 0.5$ results in a cross section of²⁴

$$\sigma(\pi)/\sigma_R(\pi) = [2\pi(2L+1)/\eta]^2 |\beta| \exp[-\lambda(\pi + \theta_L^{\text{C}})] - \Delta \exp[-\pi\Delta(\pi - \theta_L)] \exp[-i(2\pi L + \Phi_\beta - 2\delta_L)]|^2, \quad (12)$$

The small values of λ and β required by the analysis are unusual from the optical-potential point of view. Typical potential poles in the surface region are farther from the real axis and have larger residues.^{7,16} These poles are perhaps best described as "barrier top" resonances²⁰ in which a fairly unstable standing wave is produced over the barrier. Poles much closer to the real axis would indicate a more stable structure produced by an effective trapping potential in the surface region instead of a barrier—e.g., by a neck formation. These would be characteristic of quasimolecular, intermediate-structure resonances (see, e.g., Feshbach,²¹ and references therein).

On the other hand, optical-model fits have been made for $^{16}\text{O} + ^{28}\text{Si}$ backward angular distributions^{3,7,8,10}. One must therefore consider the possibility of a more conventional interpretation of the backward-angle excitation function.²² For this purpose, let us consider separating the S matrix into a nonresonant part and a resonant pole part,

$$S_l = S_l^{\text{NR}} + S_l^{\text{P}}. \quad (9)$$

The first part includes many overlapping poles and gives rise to the typical strong-absorption average behavior of S_l .¹⁵ It may be parametrized by the smooth-cutoff expression,

$$S_l^{\text{NR}} = \exp(i2\sigma_l) [1 + \exp[(L-l)/\Delta]]^{-1}, \quad (10)$$

where δ_l is the real part of the average nuclear phase shift. This expression has poles $l_n = L + in\pi\Delta$, $n = \pm 1, \pm 2, \dots$ with residues $\Delta \exp(i2\delta_{l_n})$. Thus we obtain the backward-angle diffraction amplitude produced by such a parametrization^{13,14} as

where Φ_β is the phase of the residue. The interference term is proportional to $\cos(2\pi L + \Phi_\beta - 2\delta_L)$. It gives structure with the same period as $\sin^2\pi L$ provided $\Phi_\beta - 2\delta_L$ is relatively constant. By definition, this should be so. Also note that the interference does not rely solely on Eq. (10). It should always be possible to parametrize S_i^{NR} in the vicinity of L by functions having a similar pole structure near the real axis. I conclude that the interference of resonant and nonresonant diffraction amplitudes generally produces periodic structure in backward-angle excitation functions with a frequency $\Delta E = (dL/dE)^{-1} \approx 2E/L$. Note also that if the cross section is large, then the pole contribution must dominate since Eq. (9) implies that the rapid variation of S_i resides in S_i^P .

A fit to the data with Eq. (12) is shown by the dashed curve in Fig. 1. Based on the types of residues found for optical potentials,^{7,16} we let $|\beta| = 0.5$. In order to have integer L values for the peaks, we set $\Phi_\beta - 2\delta_L = \pi$. (This condition is not important.) The E dependence of λ , $\lambda = 0.0325 \times E + 0.1471$, was fixed by the average cross section at two points (27.2 and 30 MeV).²⁵ Ignoring nuclear deflection, $\Delta = 1.035$ was adjusted to give the height of the 29.3-MeV peak.

Clearly, small Δ values are required to produce a significant nonresonant diffraction amplitude. A value of $\Delta = 1.2$ would remove most of the structure shown in Fig. 1. The value obtained seems to be slightly smaller than what would be expected from fitting forward-angle data with Eq. (10). Note also that the width of S_i^{NR} should increase with a \sqrt{E} dependence.²³ However, a relatively small Δ is a natural sign of a weak surface absorption and would have a more pronounced effect in the backward-angular region. Note again that the Δ in the exponent of Eq. (12) is a measure of the local variation of S_i^{NR} near L and is not necessarily fixed by the total width of S_i^{NR} .

We have seen that it is possible to explain periodic structure in backward-angle excitation functions for strongly absorbing particles in three ways. A normal, nonresonant diffraction effect could be ruled out for the case of heavy ions. An isolated, quasimolecular type of resonance is a viable explanation, but it is an extreme assumption which presently has no additional support. It is more general to consider an elastic-type resonance interfering with a diffraction background. This view is supported in the $^{16}\text{O} + ^{28}\text{Si}$ case by optical-model calculations. Because of the sensitivity to the background, it

is important to note the limit in which a moderate pole completely dominates the backward-angle scattering. This case would show large oscillatory angular distributions but no structure in the backward-angle excitation function.

Concerning the angular distributions, one needs only to include the appropriate $P_l[\cos(\pi-\theta)]$ factors in Eqs. (6) and (11) to describe the far-backward region. More significantly, there are closed formulas for the normal diffraction amplitude at all angles.²³ Thus it should be possible to study the pole-background interference all the way to the forward angles ($\theta \gtrsim \theta_L$) where the normal diffraction dominates. In this way the various parameters could be pinned down at fixed energies.

It is a pleasure to thank K. A. Eberhard, W. E. Frahn, K. M. Hartmann, and H. H. Wolter for helpful discussions. This work has supported by the Bundesministerium für Kernforschung und Technologie, Federal Republic of Germany.

¹P. Braun-Munzinger *et al.*, Phys. Rev. Lett. **38**, 944 (1977).

²See, for example, Proceedings of the Symposium on Heavy Ion Elastic Scattering, Rochester, 1977, edited by R. M. DeVries (to be published).

³V. Shkolnik *et al.*, Phys. Lett. **74B**, 195 (1978).

⁴J. Barrette *et al.*, Phys. Rev. Lett. **40**, 445 (1978).

⁵M. R. Clover *et al.*, Phys. Rev. Lett. **40**, 1008 (1978).

⁶D. Dehnhard *et al.*, Phys. Rev. Lett. **40**, 1549 (1978).

⁷T. Takemasa and T. Tamura, Phys. Rev. C **18**, 1282 (1978).

⁸S. Y. Lee, Univ. of Washington Report No. RLO-1388-753, 1978 (to be published).

⁹T. R. Renner *et al.*, Phys. Rev. C **18**, 1927 (1978).

¹⁰K. O. Terenetski and J. D. Garrett, Phys. Rev. C **18**, 1944 (1978).

¹¹V. M. Strutinsky, Z. Phys. **A289**, 65 (1978).

¹²N. Takigawa and S. Y. Lee, Nucl. Phys. **A292**, 173 (1977).

¹³E. V. Inopin, Zh. Eksp. Teor. Fiz. **48**, 1620 (1965) [Sov. Phys. JETP **21**, 1090 (1965)].

¹⁴T. E. O. Ericson, in *Preludes in Theoretical Physics*, edited by A. de Shalit, H. Feshbach, and L. van Hove (North-Holland, Amsterdam, 1966), p. 321.

¹⁵K. W. McVoy, Phys. Rev. C **3**, 1104 (1971); J. T. Londergan and K. W. McVoy, Nucl. Phys. **A201**, 390 (1973).

¹⁶T. Tamura and H. H. Wolter, Phys. Rev. C **6**, 1976 (1972).

¹⁷R. C. Fuller, Nucl. Phys. **A216**, 199 (1973).

¹⁸R. C. Fuller, Phys. Rev. C **16**, 1865 (1977).

¹⁹The energy dependences assumed should not hold down to the barrier (~ 17 MeV) where the background

integral must become dominant.

²⁰W. A. Friedman and C. J. Goebel, *Ann. Phys. (N.Y.)* **104**, 145 (1977).

²¹H. Feshbach, in *Proceedings of the International Conference on Nuclear Physics, Munich, 1973*, edited by J. de Boer and H. J. Mang (North-Holland, Amsterdam, 1973), p. 632.

²²The approach in Ref. 8 relies on an interior wave contribution. This is outside the strong-absorption

framework which is considered here.

²³W. E. Frahn and H. Venter, *Ann. Phys. (N.Y.)* **24**, 243 (1963); W. E. Frahn and D. H. E. Gross, *Ann. Phys. (N.Y.)* **101**, 520 (1976).

²⁴For simplicity, let the L of Eq. (10) correspond to the real part of the resonant pole position.

²⁵The resulting value of $\lambda = 1.28$ at 35 MeV is close to the values found in Ref. 7 for potential fits to the corresponding angular distribution.

Irregularities in Side-Feeding Patterns, Energies, and Multipolarities in the ^{154}Er Yrast Cascade to Spin 36

C. Baktash, E. der Mateosian, O. C. Kistner, and A. W. Sunyar
Brookhaven National Laboratory, Upton, New York 11973

(Received 9 October 1978)

States of ^{154}Er were studied by means of the ($^{16}\text{O}, 4n$) and ($^{64}\text{Ni}, 4n$) reactions. Beginning with a 40-nsec isomeric state [$J^\pi = (10^-, 11^-)$], an intensely populated unusual cascade of $\Delta J = 2$ and $\Delta J = 1$ transitions was established up to spin (35, 36) and 12.5 MeV excitation. On an E vs $I(I+1)$ plot the yrast levels form a series of straight-line segments with side feeding occurring primarily at the ends of segments. A second cascade of even-spin, even-parity levels from the ground state to $J^\pi = 18^+$ (quasi-ground-state band) does not exhibit these properties.

Interesting data generated in part by searches for high-spin isomeric states,¹ or "yrast traps," have recently appeared for nuclei with $A \approx 150$. Calculations² predict oblate shapes for $I < 40$ in nuclei with neutron number $N = 84-88$, making this a likely region for yrast traps. Isomers have been found here, and an isomeric state has been reported in ^{154}Er by Aguer *et al.*³

The present work confirms part of the decay scheme of ^{154}Er as presented in Ref. 3, but it reorders several transitions and assigns spins to some low-lying levels. A quasi-ground-state band is extended beyond the previous highest spin state (14^+) to spin 18^+ and, most importantly, a high-spin yrast cascade is extended by six levels up to spin (35, 36) and excitations over 12 MeV. The detailed structure of the yrast cascade differs significantly from an yrast cascade reported by Khoo *et al.*⁴ from spin (36, 37) in the $N = 86$ isotope ^{152}Dy . The present study of ^{154}Er extends our investigations of high-spin states from the deformed "rotational" Er nuclei⁵ down through the transitional region⁶ to the near-closed-shell nuclei.

^{154}Er was produced by means of the reactions ($^{16}\text{O}, 4n$) on ^{142}Nd at 95-102 MeV and ($^{64}\text{Ni}, 4n$) on ^{94}Zr at 270 and 275 MeV. Targets of ^{142}Nd (4 mg/cm²) and ^{94}Zr (3 mg/cm²) were backed with ^{208}Pb . Ge-Li detectors with $\sim 15\%$ efficien-

cies and ~ 2 -keV resolution at 1.33 MeV were used for γ - γ coincidence and angular-distribution studies. A pulsed ^{16}O beam was used to obtain delayed γ spectra, and some results of these measurements are shown in Fig. 1. A decay scheme based on these data is shown in Fig. 2.

The sequence of states in the quasi-ground-state band up to spin 18^+ was inferred from singles and coincidence data. Angular distributions for these transitions are consistent with a cascade of stretched $E2$'s. This cascade is composed of transitions which up to level 16^+ do not differ more than $\pm 12\%$ from a mean energy of 615 keV. A 432- and 796-keV side cascade of transitions feeds into the 6^+ level. Angular-distribution data are consistent with a $\Delta J = 1$ and a $\Delta J = 2$ assignment to the 432- and 796-keV transitions, respectively. This sequence is characterized as proceeding between levels with spin $9^- \rightarrow 8^+ \rightarrow 6^+$. The order is established by a weak 254-keV transition which takes place between the 8^+ level and the 8^+ member of the quasi-ground-state band. A parallel sequence, 554 keV ($\Delta J = 2$) and 674 keV ($\Delta J = 1$), originates at the spin-9 level, ends at the 6^+ state, and is thus characterized as being $9^- \rightarrow 7^- \rightarrow 6^+$. A third transition, 686.5 keV ($\Delta J = 1$), originates at the 9 level and proceeds to the 8^+ level of the quasi-ground-state band.